Charge detection in graphene quantum dots

J. Güttinger,[a] C. Stampfer, S. Hellmüller, F. Molitor, T. Ihn, and K. Ensslin
Solid State Physics Laboratory, ETH Zurich, 8093 Zurich, Switzerland

(Received 17 September 2008; accepted 5 November 2008; published online 24 November 2008)

We report measurements on a graphene quantum dot with an integrated graphene charge detector. The quantum dot device consists of a graphene island (diameter of ~200 nm) connected to source and drain contacts via two narrow graphene constrictions. From Coulomb diamond measurements a charging energy of 4.3 meV is extracted. The charge detector is based on a 45 nm wide graphene nanoribbon placed approximately 60 nm from the island. We show that resonances in the nanoribbon can be used to detect individual charging events on the quantum dot. The charging induced potential change on the quantum dot causes a steplike change in the current in the charge detector. The relative change in the current ranges from 10% up to 60% for detecting individual charging events. © *2008 American Institute of Physics*. [DOI: 10.1063/1.3036419]

Graphene,[1,2] the two dimensional (2D) sp^2 allotrope of carbon, is a promising material for the development of future nanoelectronics and quantum information processing.[3] This is mainly due to high carrier mobilities[4,5] and expected long spin lifetimes. Graphene's gapless electronic structure and predicted Klein tunneling through *pn* barriers[6] make it hard to confine charge carriers by electrostatic means. However, by etching graphene it is possible to make tunable graphene nanodevices, as it has been shown by the fabrication of graphene nanoribbons,[7–9] interference devices,[10–12] and graphene quantum dots (QDs).[13–15] In this paper we present an integrated graphene device consisting of a graphene QD with a nearby graphene nanoribbon acting as a quantum-point-contact-like charge detector (CD). Charge detection techniques[16] have been shown to significantly extend the experimental possibilities with QD devices. They are, e.g., powerful for detecting spin-qubit states[17,18] and molecular states in coupled QDs.[19] Furthermore CDs have been successfully used to investigate shot noise on a single electron level and full counting statistics.[20] This makes charge detection highly interesting for advanced investigation of graphene QDs and graphene nanosystems in general.

Figure 1(a) shows a scanning force microscope image of the all graphene structure. The QD device consists of two 35 nm wide graphene constrictions separating source (*S*) and drain (*D*) contacts from the graphene island (diameter of ~200 nm). The constrictions and the island are electrostatically tuned independently by two barrier gates (B1 and B2) and a plunger gate (PG), respectively. The highly doped silicon back gate (BG) allows to adjust the overall Fermi level. In addition, we placed a 45 nm wide graphene nanoribbon 60 nm next to the island, which acts as a CD, as shown below.

The sample is fabricated by mechanical exfoliation of natural bulk graphite.[21] Single-layer graphene flakes are transferred to highly doped silicon substrates with a 295 nm silicon oxide top layer. Electron beam lithography (EBL) is used for patterning the isolated graphene flakes by subsequent Ar/O_2 reactive ion etching. A second EBL and a lift-off step is performed to place source, drain electrodes, and contacts to the lateral gate electrodes (all 2/50 nm Ti/Au). For the detailed fabrication process and the single-layer graphene identification by Raman spectroscopy, we refer to Refs. 13, 22, and 23. Measurements were performed in a variable temperature insert cryostat at a base temperature of 1.7 K using low-frequency lock-in techniques.

The characterization of the individual devices is shown in Figs. 1(b) and 1(c). Figure 1(b) shows the current I as a function of the BG voltage at a temperature of 1.7 K of both the QD device (upper curve) and the CD (lower curve). In both cases we observe a transport gap[13] extending roughly from −4 to 15 V and from 4 to 14 V for the QD and CD, respectively. From high source-drain voltage ($V_{b,\mathrm{QD}}$) measurements (not shown) we estimate the characteristic energy scale of these effective energy gaps to be about 13 and 8 meV, respectively. This is in reasonable agreement with recent measurements on graphene nanoribbons, where the transport gap is dominated by the width of the graphene nanostructure.[24] The large scale current fluctuations are attributed to resonances in the graphene constrictions. By focusing on a smaller BG voltage range of 150 mV [see inset of Fig. 1(b)], Coulomb blockade resonances of the QD are resolved in regions where these resonances are suppressed. In Fig. 1(c) Coulomb diamond measurements of the QD are shown. The differential conductance of the dot $dI_{\mathrm{QD}}/dV_{b,\mathrm{QD}}$ is plotted as a function of the bias voltage $V_{b,\mathrm{QD}}$ and PG voltage V_{PG} for a fixed BG voltage $V_{\mathrm{BG}}=2$ V. From this measurement a charging energy $E_c \approx 4.3$ meV and a PG lever arm $\alpha_{\mathrm{PG,QD}}=0.06$ are extracted. From further diamond measurements as function of BG and fixed PG voltage (not shown here), we find a BG lever arm of $\alpha_{\mathrm{BG,QD}}=0.34$. After having demonstrated the functionality of both devices independently, their joint operation is shown in Figs. 2 and 3, where we demonstrate the functionality and high sensitivity of the graphene CD.

For these measurements the BG voltage is set to $V_{\mathrm{BG}}=6.5$ V such that the QD is close to the charge neutrality point [see arrows in Fig. 1(b)] as well as inside the transport gap of the CD. We operate the CD in a regime where strong resonances are accessible in order to make use of steep slopes of the conductance as a function of V_{PG} of the order of $4-6\times10^{-4}(e^2/h)/100$ mV to detect individual charging events on the QD.

[a]Electronic mail: guettinj@phys.ethz.ch.

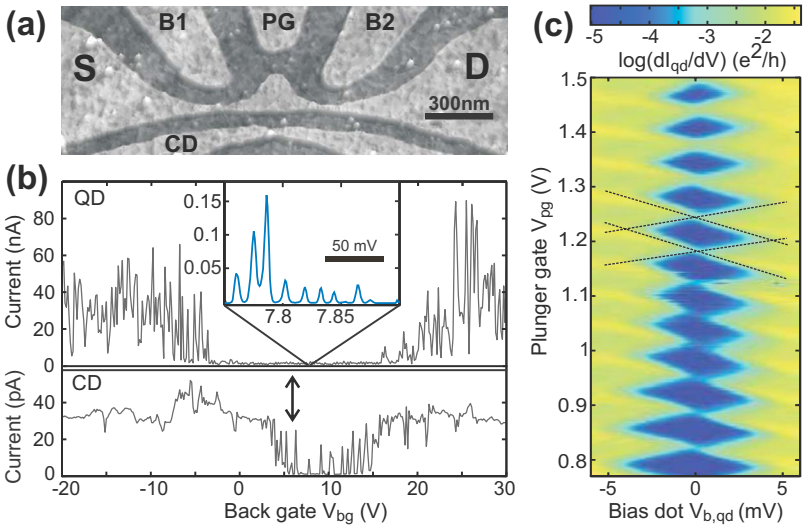

FIG. 1. (Color online) Nanostructured graphene QD device with nanoribbon and characteristic transport measurements. (a) Scanning force micrograph of the measured device. The central island is connected to source (S) and drain (D) contacts by two constrictions. The diameter of the dot is 200 nm and the constrictions are 35 nm wide. The graphene nanoribbon acts as CD. Three lateral gates B1, B2, and PG are used to tune the devices. (b) BG characteristics of the QD device (upper panel) and the CD (lower panel) shown in (a). Both measurements were performed at a source-drain (bias) voltage of $V_{b,\mathrm{QD}}=V_{b,\mathrm{CD}}=500\ \mu\mathrm{V}$ and at 1.7 K. The inset shows Coulomb blockade resonances observed inside the transport gap as a function of the BG voltage over a range of 150 mV. (c) Coulomb blockade diamonds in differential conductance (logarithmic scale) recorded as function of the PG and bias voltage with fixed BG voltage $V_{\mathrm{BG}}=2$ V. The charging energy is estimated to be $E_c\approx 4.3$ meV.

Figure 2(a) shows almost equidistantly spaced ($\Delta V_{\mathrm{PG}}=65\pm 3.8$ mV) Coulomb blockade resonances as function of V_{PG} at $V_{b,\mathrm{QD}}=500\ \mu$V. The strong modulation of the conductance peak amplitudes is due to superimposed resonances in the graphene constrictions defining the island.[13] In Fig. 2(b) we plot the simultaneously measured conductance through the nearby CD (at a bias voltage of $V_{b,\mathrm{CD}}=8.2$ mV) for the same V_{PG} range. On top of the peak-shaped CD resonance we observe conductance steps that are well aligned (see dotted lines) with single charging events on the nearby QD. The conductance step is related to a shift in the CD resonance with respect to the PG voltage. From an analysis of more than 300 charging events an average shift in PG voltage of $\Delta V_{\mathrm{PG,CD}}=34\pm 6$ mV is observed. Despite the fact that in Fig. 2(b) the shifts are larger for lower PG voltage, no systematic dependence on the PG voltage or on the dot conductance or on the individual CD resonance can be extracted.

Figures 3(a) and 3(b) show 2D plots of a set of traces corresponding to those shown in Figs. 2(a) and 2(b) taken for different BG voltages and $V_{b,\mathrm{CD}}=V_{b,\mathrm{QD}}=500\ \mu$V. Figure 3(a) shows Coulomb blockade resonances in the QD conductance following a relative lever arm of PG and BG of $\alpha_{\mathrm{PG,QD}}/\alpha_{\mathrm{BG,QD}}=0.18$ (see black dashed line). In Fig. 3(b) these resonances are observed through charge detection and are marked with arrows. The CD resonance used for detection can be distinguished from the dot resonances by its larger width and its different slope given by $\alpha_{\mathrm{PG,CD}}/\alpha_{\mathrm{BG,CD}}=0.04$ (black dashed line). This reduced slope is due to the larger distance of the CD nanoribbon to the PG ($\sim$350 nm) as compared to the island-PG distance. The modulation of the Coulomb blockade resonances in Fig. 3(a) is due to resonances in the tunneling constriction located around 300 nm away from the PG [see Fig. 1(a)]. This leads to a slope of 0.08 for these peak modulations (see white dotted line). Independent of this modulation we identify single charging events on the QD as conductance fringes [see arrows in Fig. 3(b)] on top of the up and down slopes of the CD resonance. This can even better be seen by numerical differentiation of G_{CD} versus V_{PG}, as shown in Fig. 3(c). Here the sharp conductance changes due to the fact that charging events in the dot are strongly pronounced, and both relative lever arms to the Coulomb blockade peaks and the constriction resonance in the CD are indicated by dashed lines. The detection range can be improved by increasing the bias $V_{b,\mathrm{CD}}$, leading to a broadening of the constriction resonance, as seen by comparing Fig. 3(c) with Fig. 2(b).

From the measurement shown in Fig. 2(b) a nanoribbon conductance change of up to 10% can be extracted for a single charging event. For lower bias voltages (e.g., $V_{b,\mathrm{CD}}=500\ \mu$V) the change in the conductance can be increased to 60%.

In conclusion, we demonstrated the functionality of an integrated graphene CD based on a nanoribbon nearby a graphene QD. We confirm the detection of charging events in regimes where Coulomb blockade resonances can hardly be measured (i.e., resolved) because the current levels are too low [see, e.g., arrows in Fig. 2(a)]. In contrast to state-of-the-art quantum-point contact CDs, we do not make use of slopes to quantized conductance plateaus. We rather use local resonances in the graphene nanoribbon to detect charging. We anticipate that this technique will play an important role for the investigation of the electron-hole crossover and spin states in graphene QDs.

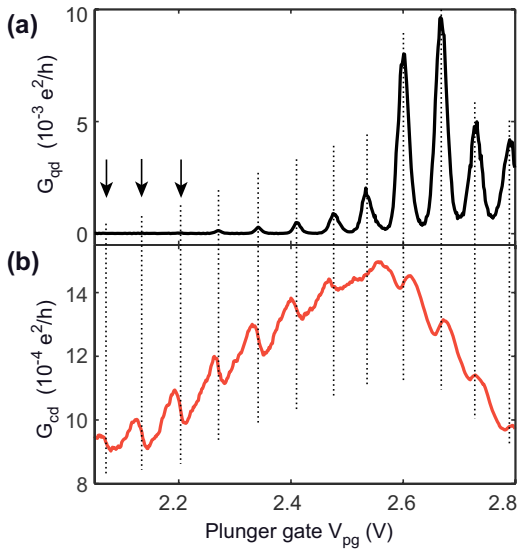

FIG. 2. (Color online) (a) Dot conductance G_{QD} and (b) CD conductance G_{CD} as a function of PG voltage V_{PG} for a fixed BG voltage $V_{\mathrm{BG}}=6.5$ V. (a) The arrows indicate Coulomb blockade resonances that can be hardly measured by conventional means because the current levels are too low. (b) However, they can be detected by the CD. Bias on dot: $V_{b,\mathrm{QD}}=500\ \mu$V. Bias on CD: $V_{b,\mathrm{CD}}=8.2$ mV.

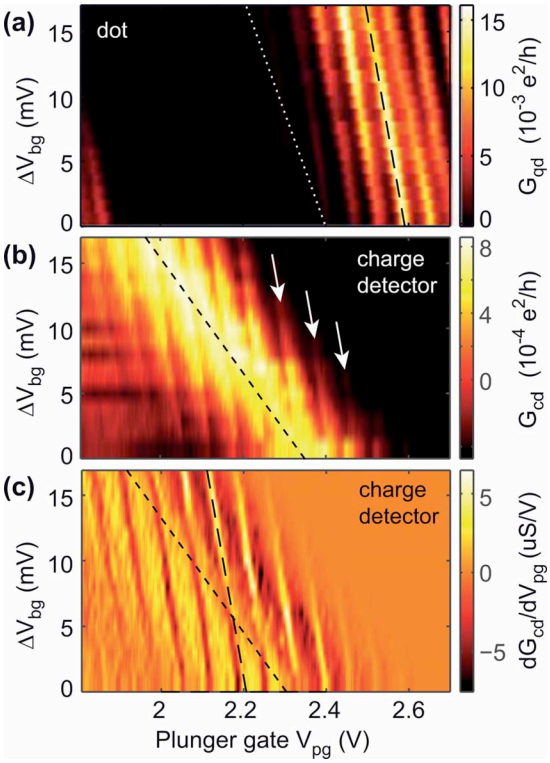

FIG. 3. (Color online) (a) Conductance G_{QD} of the QD as a function of PG voltage V_{PG} and BG voltage V_{BG}. The BG voltage is converted to a relative scale starting at V_{BG}=6.505 V with ΔV_{BG}=0. For this measurement a source-drain bias of $V_{b,QD}$=500 μV is symmetrically applied. Narrowly spaced periodic lines are Coulomb blockade resonances (black line with long dashes), while the larger scale features are attributed to a modulation of the transmission through the barriers (white dotted line). (b) Simultaneous measurement of the CD conductance G_{CD}. The broad line with increased conductance is less affected by changing the PG voltage compared to the Coulomb blockade resonances in the dot, and it is attributed to a local resonance in the CD (short dashed line). In addition to this broad line, faint lines with a slope corresponding to the Coulomb blockade resonances in the QD are observed (arrows). (c) Derivative of the CD conductance is plotted in (b) with respect to PG voltage dG_{CD}/dV_{PG}, where the lines with short and long dashes indicate the two different lever arms.

The authors wish to thank R. Leturcq, P. Studerus, C. Barengo, P. Strasser, A. Castro-Neto, and K. S. Novoselov for helpful discussions. Support by the ETH FIRST Laboratory, the Swiss National Science Foundation, and NCCR nanoscience is gratefully acknowledged.

[1] A. K. Geim and K. S. Novoselov, Nature Mater. **6**, 183 (2007).
[2] M. I. Katsnelson, Mater. Today **10**, 20 (2007).
[3] B. Trauzettel, D. V. Bulaev, D. Loss, and G. Burkard, Nat. Phys. **3**, 192 (2007).
[4] K. S. Novoselov, A. K. Geim, S. V. Morozov, D. Jiang, M. I. Katsnelson, I. V. Grigorieva, S. V. Dubonos, and A. A. Firsov, Nature (London) **438**, 197 (2005).
[5] Y. Zhang, Y.-W. Tan, H. L. Stormer, and P. Kim, Nature (London) **438**, 201 (2005).
[6] M. I. Katsnelson, K. S. Novoselov, and A. K. Geim, Nat. Phys. **2**, 620 (2006).
[7] Z. Chen, Y. Lin, M. Rooks, and P. Avouris, Physica E (Amsterdam) **40**, 228 (2007).
[8] M. Y. Han, B. Özyilmaz, Y. Zhang, and P. Kim, Phys. Rev. Lett. **98**, 206805 (2007).
[9] X. Li, X. Wang, L. Zhang, S. Lee, and H. Dai, Science **319**, 1229 (2008).
[10] F. Miao, S. Wijeratne, Y. Zhang, U. C. Coskun, W. Bao, and C. N. Lau, Science **317**, 1530 (2007).
[11] S. Russo, J. B. Oostinga, D. Wehenkel, H. B. Heersche, S. S. Sobhani, L. M. K. Vandersypen, and A. F. Morpurgo, Phys. Rev. B **77**, 085413 (2008).
[12] F. Molitor, M. Hüfner, A. Jacobsen, A. Pioda, C. Stampfer, T. Ihn, and K. Ensslin (unpublished).
[13] C. Stampfer, J. Güttinger, F. Molitor, D. Graf, T. Ihn, and K. Ensslin, Appl. Phys. Lett. **92**, 012102 (2008).
[14] C. Stampfer, E. Schurtenberger, F. Molitor, J. Güttinger, T. Ihn, and K. Ensslin, Nano Lett. **8**, 2378 (2008).
[15] L. A. Ponomarenko, F. Schedin, M. I. Katsnelson, R. Yang, E. H. Hill, K. S. Novoselov, and A. K. Geim, Science **320**, 356 (2008).
[16] M. Field, C. G. Smith, M. Pepper, D. A. Ritchie, J. E. F. Frost, G. A. C. Jones, and D. G. Hasko, Phys. Rev. Lett. **70**, 1311 (1993).
[17] J. R. Petta, A. C. Johnson, J. M. Taylor, E. A. Laird, A. Yacoby, M. D. Lukin, C. M. Marcus, M. P. Hanson, and A. C. Gossard, Science **309**, 2180 (2005).
[18] J. M. Elzerman, R. Hanson, L. H. Willems van Beveren, B. Witkamp, L. M. K. Vandersypen, and L. P. Kouwenhoven, Nature (London) **430**, 431 (2004).
[19] L. DiCarlo, H. Lynch, A. Johnson, L. Childress, K. Crockett, C. Marcus, M. Hanson, and A. Gossard, Phys. Rev. Lett. **92**, 226801 (2004).
[20] S. Gustavsson, R. Leturcq, B. Simovic, R. Schleser, T. Ihn, P. Studerus, and K. Ensslin, Phys. Rev. Lett. **96**, 076605 (2006).
[21] K. S. Novoselov, A. K. Geim, S. V. Morozov, D. Jiang, M. I. Katsnelson, S. V. Dubonos, I. V. Grigorieva, and A. A. Firsov, Science **306**, 666 (2004).
[22] A. C. Ferrari, J. C. Meyer, V. Scardaci, C. Casiraghi, M. Lazzeri, F. Mauri, S. Piscanec, D. Jiang, K. S. Novoselov, S. Roth, and A. K. Geim, Phys. Rev. Lett. **97**, 187401 (2006).
[23] D. Graf, F. Molitor, K. Ensslin, C. Stampfer, A. Jungen, C. Hierold, and L. Wirtz, Nano Lett. **7**, 238 (2007).
[24] F. Sols, F. Guinea, and A. H. Castro Neto, Phys. Rev. Lett. **99**, 166803 (2007).